Nanopropellers and Their Actuation in Complex Viscoelastic Media

Debora Schamel,[†,‡] Andrew G. Mark,[†] John G. Gibbs,[†] Cornelia Miksch,[†] Konstantin I. Morozov,[§] Alexander M. Leshansky,[§] and Peer Fischer[†,‡,*]

[†]Max Planck Institute for Intelligent Systems, Heisenbergstraße 3, 70569 Stuttgart, Germany, [‡]Institute for Physical Chemistry, University of Stuttgart, Pfaffenwaldring 55, 70569 Stuttgart, Germany, and [§]Department of Chemical Engineering and Russel Berrie Nanotechnology Institute, Technion, Haifa 32000, Israel

ABSTRACT Tissue and biological fluids are complex viscoelastic media with a nanoporous macromolecular structure. Here, we demonstrate that helical nanopropellers can be controllably steered through such a biological gel. The screw-propellers have a filament diameter of about 70 nm and are smaller than previously reported nanopropellers as well as any swimming microorganism. We show that the nanoscrews will move through high-viscosity solutions with comparable velocities to that of larger micropropellers, even though they are so small that Brownian forces suppress their actuation in pure water. When actuated in viscoelastic hyaluronan gels, the nanopropellers appear to have a significant advantage, as they are of the same size range as the gel's mesh size. Whereas larger helices will show very low or negligible propulsion in hyaluronan solutions, the nanoscrews actually display significantly enhanced propulsion velocities that exceed the highest measured speeds in Newtonian fluids. The nanopropellers are not only promising for applications in the extracellular environment but small enough to be taken up by cells.

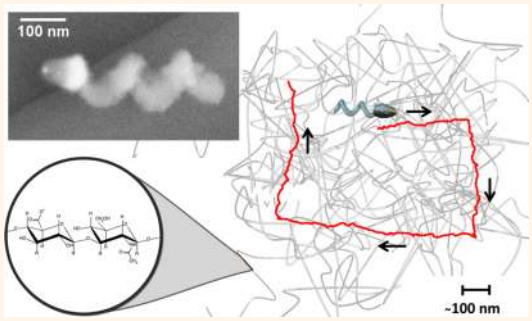

KEYWORDS: micropropulsion · viscoelastic fluids · polymeric networks · magnetic actuation · Brownian motion · vapor deposition · glancing angle deposition

Magnetically actuated helical micropropellers have attracted considerable attention over the past couple of years due to their ability to propel with high precision on a micrometer length scale without requiring chemical fuel.[1−5] These qualities make them particularly promising for biological and biomedical applications.[6,7] Most demonstrations of their propulsion capabilities have been performed in water or other Newtonian fluids. However, to realize applications inside living organisms, these propellers must also move through biological materials, which are generally very complex rheological systems exhibiting non-Newtonian, size-dependent, and viscoelastic behaviors.

Many microorganisms swim through viscoelastic polymeric solutions, applying a variety of propulsion mechanisms that can result in both enhancement and retardation of swimming speeds compared to Newtonian liquids.[8−13] The movement of artificial microswimmers in viscoelastic solutions has been studied both theoretically and experimentally.[14−18] The behavior can be complex. For instance, when moving in Boger-fluid, the force-free swimming speed of a macroscale rigid helix can be both faster and slower than in Newtonian fluids, depending on the drive frequency relative to the elastic relaxation time.[14] For heterogeneous gel-like media with a mesh size larger than the swimmer size, enhanced propulsion was demonstrated theoretically.[16,18]

Biological fluids often contain a high amount of macromolecules, cells, and other colloidal structures, which influence the medium's rheological properties. Blood, for example, contains high concentrations of dispersed cells, which for a microscale swimmer act as rigid obstacles. Nevertheless, micropropellers have been successfully steered through undiluted blood samples and were found to undergo stick−slip motion.[19]

However, many biological media contain fluids of a more challenging type: dense gel-like networks of interconnected polymer chains with mesh sizes in the range of tens to hundreds of nanometers.[20−22] The result is that motion for particles larger than the mesh size is impeded, while smaller particles pass through the mesh with little resistance. Thus, such media are characterized

* Address correspondence to fischer@is.mpg.de.

Received for review April 30, 2014 and accepted June 9, 2014.

Published online June 09, 2014
10.1021/nn502360t

by strongly size-dependent transport behavior of both molecules and nanoparticles.[23−26]

Hyaluronan (HA) presents an excellent model for a mesh-like biologically relevant medium. It occurs at low concentrations throughout the human body, in both the extra- and intracellular matrices. HA is high in concentration in the synovial fluid of the joint and in the vitreous humor of the eye, where it contributes to the medium's viscoelastic properties, and controls tissue hydration and water transport, among other functions.[22,27−29] The mesh structure of HA that accounts for the polymer's mechanical properties is highly permeable to small molecules, but it hinders the transport of larger particles, and has been suggested as a suitable model for various material transport phenomena in biological systems.[23] Even though it has been shown that helical propellers should, from a hydrodynamic viewpoint, be able to propel in viscoelastic media, the problem that arises with magnetically actuated micrometer-scale propellers is that in these biological polymer solutions mesh entanglement results in an effective resistance that is significantly higher than in water. Therefore, the torque that can be applied with realistic laboratory magnetic fields is insufficient for effective propulsion. For example, our observations show that even in relatively dilute solutions of HA, micropropellers of the size studied to date, with diameters of about 400 nm or above,[1,4,30] do not effectively move.

Enhanced diffusion for passive spherical nanoparticles below the mesh size has been previously observed in various biological tissues.[25,31] This suggests that one strategy for avoiding mesh entanglement is to simply reduce the propeller size to dimensions comparable to the openings in the polymer network, *i.e.*, to the nanoscale (see Figure 1). This poses two challenges: fabricating the complex shape and realizing the multifunctional material composition necessary for the propeller, and successfully steering the propeller in a size regime where diffusive Brownian motion typically dominates.[30] Propellers this small are of interest not only because they would be capable of locomotion and operation in extracellular biological fluids, but also because they could potentially perform tasks inside living cells.

Here, we report what to our knowledge are the smallest magnetically actuated propellers to date with a filament diameter of approximately 70 nm. We demonstrate that these nanoscrews not only are able to move through HA solutions but even show enhanced propulsion in HA gels compared to their movement in purely viscous solutions. Furthermore, the difficulties of propelling helices this small in Newtonian fluids are addressed. We show in a theoretical analysis how the effect of thermal noise scales with the propeller's size, the fluid's viscosity, and the rotational frequency, which enables us to estimate the minimum size a screw-propeller must have in order to successfully move in a solution of a given viscosity. The theoretical results agree well with our experimental observations: the nanopropellers cannot be effectively propelled in water, but will show efficient directional motion in solutions with higher viscosities.

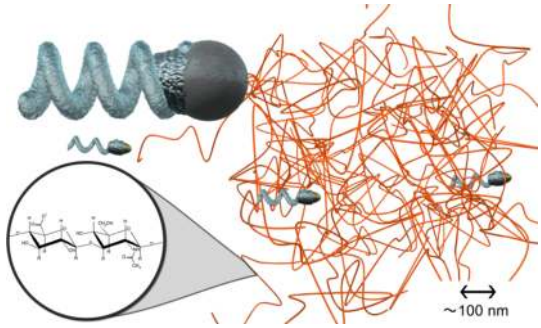

Figure 1. Schematic of micro- and nanopropellers in hyaluronan gels. The polymeric mesh structure hinders the larger helices from translating effectively, whereas smaller propellers with a diameter close to the mesh size can pass through the network without being affected by the macroscopic viscoelasticity caused by the entangled polymer chains.

RESULTS AND DISCUSSION

The nanopropellers are produced using a recently published shadow-growth technique on nanolithographically patterned substrates.[32] Silica helices containing a Ni-segment for magnetic propulsion were grown at room temperature using glancing angle deposition (GLAD)[33−36] on top of uniform arrays of Au nanodots produced *via* micellar nanolithography[37] with spacings around 135 nm. The magnetic nickel section has a thickness of about 40 nm, and the helices have a filament diameter of roughly 70 nm and a total width of up to 120 nm. They are approximately 400 nm long and have a pitch of 100 nm. They are therefore around 3 to 4 times smaller in every dimension than the smallest functioning helical propellers reported to date, which are approximately 300 nm wide and 1.5 μm long.[1] Figure 2 shows the nanopropellers on the wafer, as well as next to a 450 nm wide and 2.5 μm long micropropeller of the kind generally used by our and other groups,[4,30,38] which serves as a reference in this work. To render the helices visible in the light microscope, they were functionalized with quantum dots prior to propulsion experiments.

We performed SQUID measurements to characterize the helices' magnetic behavior. For this, the screws were magnetized in plane (IP) on the wafer and the initial magnetization was later determined at zero field both IP and out of plane (OOP). The IP magnetization was 1.13×10^{-6} emu/mm^2, whereas the OOP magnetization was only 0.13×10^{-6} emu/mm^2, so the screws are effectively diametrically magnetized. The hysteresis curves both IP and OOP can be seen in Figure 3. The saturation magnetization is roughly equal for both

orientations. The coercive field is also the same in both directions, about 65 Oe. The remnant magnetization, however, is much higher IP than OOP (about 1.3 × 10^{-6} emu/mm^2 compared to 0.4 × 10^{-6} emu/mm^2), and a clear preference for diametrical magnetization can be seen, since the permeability is significantly higher IP than OOP over a wide range of field strengths. Thus, the easy axis of magnetization is orthogonal to the helix axis (diametrical), which is optimal for converting drive torque from the external magnetic field into forward propulsion.

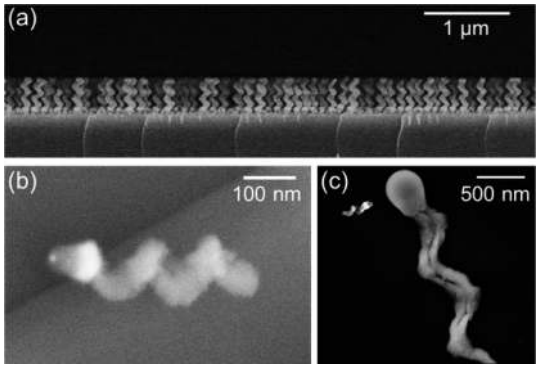

Figure 2. SEM images of the nanopropellers: (a) side view on wafer; (b) close-up of one nanohelix with both the Au-dot and the Ni-section clearly visible; image taken with an SE2 detector; (c) size comparison between the nano- and the microscrews used as a reference in this work.

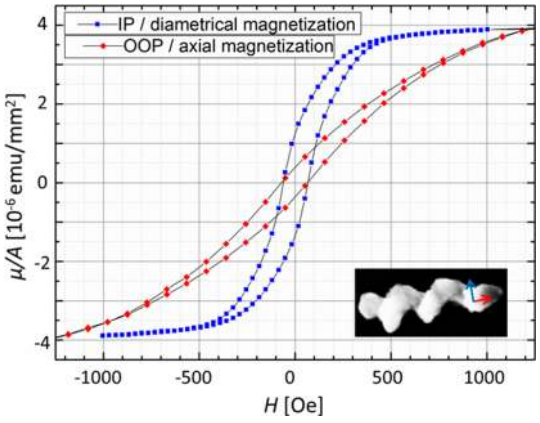

Figure 3. Magnetic hysteresis curves for nanopropellers measured on the wafer in plane (IP) and out of plane (OOP). The magnetization is given per unit surface area of the wafer, on which the screws are oriented with their long axis normal to the surface. The inset shows the respective axes marked on a propeller.

We performed our propulsion experiments with strong magnetic fields ($H \approx 100$ Oe) above the coercive (anisotropy) field ($H_a \approx 65$ Oe). Generally, one could expect helix remagnetizing at this amplitude of the external magnetic field. However, at frequencies of the rotating field below the step-out value, we do see effective propulsion and therefore conclude that the helix rotates synchronously. This behavior is plausible if the energy of remagnetization exceeds that for rotation. In fact, synchronous rotation with a magnetic field has been found for superparamagnetic beads in a frequency range similar to what we used in our study (see SI for details).[39]

Ghosh *et al.* recently performed numerical simulations to determine that the minimum length a propeller can have, before Brownian motion effects dominate such that no directional movement can be observed, is about 900 nm in water.[30] In accordance with this prediction we find that our 400 nm nanoscrews show strong diffusion and no discernible propulsion in pure water. However, no experimental test or theoretical analysis has so far been made to see how this behavior might scale with the viscosity of the medium.

Table 1 shows the absolute velocities and the dimensionless propulsion velocities (the velocity normalized by the pitch of the helix and the frequency of the magnetic field) for the nano- and microscrews in water, a Newtonian glycerol–water mixture, 3 mg/mL HA, and 5 mg/mL HA, at different frequencies and a magnetic field strength of 100 Oe. One can see that for the nanohelices in a Newtonian fluid of 25 cP, the step-out frequency (above that frequency the propeller no longer follows the rotating magnetic field) is

TABLE 1. Propulsion Velocities and Dimensionless Velocities of Nano- and Micropropellers in Newtonian Fluids and Viscoelastic Hyaluronan (HA) Solutions at Different Rotation Frequencies

	nanopropellers			micropropellers	
	25 Hz	50 Hz	80 Hz	10 Hz	25 Hz
water	0[a]	0[a]	0[a]	1.10 ± 0.20 µm/s	3.27 ± 0.48 µm/s
	0[a]	*0*[a]	*0*[a]	*0.13 ± 0.02*[b]	*0.15 ± 0.02*
glycerol– water, 25 cP	0.31 ± 0.08 µm/s	0.60 ± 0.15 µm/s	0.36 ± 0.19 µm/s	1.12 ± 0.21 µm/s	0.92 ± 0.53 µm/s
	0.12 ± 0.03	*0.12 ± 0.03*	*0.05 ± 0.03*	*0.13 ± 0.02*	*0.04 ± 0.02*
HA, 3 mg/mL	0.43 ± 0.14 µm/s	1.10 ± 0.33 µm/s	1.48 ± 0.77 µm/s	0.93 ± 0.29 µm/s	0.22 ± 0.45 µm/s
	0.17 ± 0.06	*0.22 ± 0.07*	*0.19 ± 0.10*	*0.11 ± 0.03*	*0.01 ± 0.02*
HA, 5 mg/mL	0.58 ± 0.26 µm/s	1.08 ± 0.48 µm/s	1.46 ± 0.79 µm/s	0.04 ± 0.05 µm/s	
	0.23 ± 0.10	*0.22 ± 0.10*	*0.18 ± 0.10*	*0.00 ± 0.01*	

[a] Brownian motion was so strong in water that particle tracking analysis was not possible and no directed propulsion was observed under these conditions. [b] The number in italics below the speed is the dimensionless propulsion velocity, the speed normalized by the screw's pitch and the frequency of the magnetic field. One can see that the nanopropellers show higher dimensionless velocities in HA than the micropropellers.

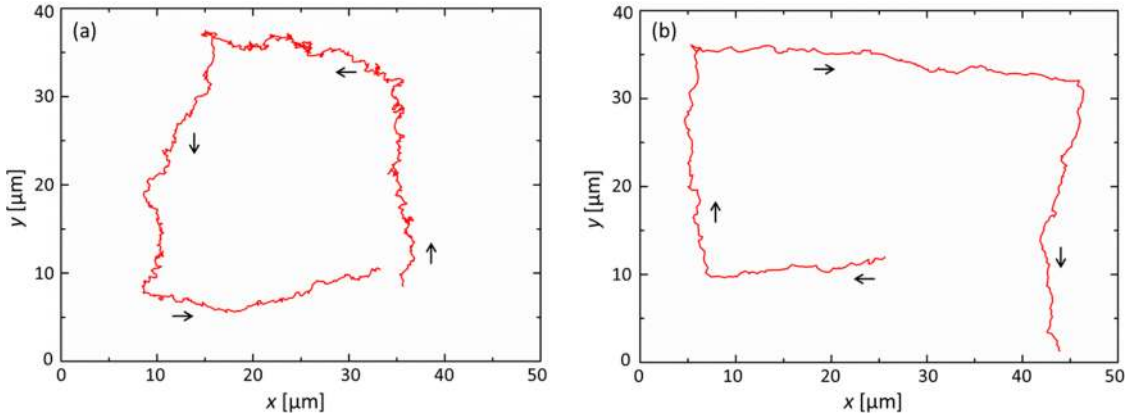

Figure 4. Tracks of nanoscrews being propelled successively in all four in-plane directions at a magnetic field strength of 100 Oe and a frequency of 50 Hz, in (a) a glycerol−water mixture with a viscosity of about 25 cP, recorded over 170 s, and (b) a 5 mg/mL HA solution, recorded over 70 s. Arrows indicate the direction of propulsion.

reached between 50 and 80 Hz (the theoretically estimated value of the step-out frequency is ~73 Hz; see SI), resulting in a significantly reduced dimensionless velocity. This value is considerably higher than that for the micropropellers. Below the step-out frequency, however, both propeller types translate with comparable dimensionless velocities. A typical track of a nanopropeller can be seen in Figure 4a. The corresponding video can be found in the SI.

HA displays much more complicated rheological properties than purely viscous glycerol solutions, as it is a highly viscoelastic material above the entanglement concentration.[40−42] In aqueous solution HA forms a transient, extended network of overlapping HA chains, which has been studied using pulsed field gradient NMR,[23] electron microscopy,[43] light scattering,[44] and probe diffusion experiments.[24] The mesh size is generally agreed on to be in the size range of tens of nanometers, with slight variations depending on the HA concentration, molecular weight, and salt concentration.

The viscoelasticity of our HA samples is relatively low, which complicates high-precision measurements using a rheometer, but our estimates from rheological measurements place the complex viscosity in the range of hundreds of cP (depending on shear rate). This is in good agreement with values reported by other groups.[29,45] The value is much higher than the viscosity of the water−glycerol mixture we used, which underlies the micropropellers' inability to move through these solutions. However, since these measurements do not reveal anything about the rheological properties at the length scale of the (nano-) propellers—a length scale close to the network size—we label the solutions by their respective concentration.

In 3 mg/mL HA, which corresponds roughly to the HA concentration found in synovial fluid,[22] the micropropellers are still able to move at a comparable speed to that in Newtonian fluids, although they experience a much higher viscous drag than in pure water, which results in a very low step-out frequency (<25 Hz). When the concentration is increased only slightly, to 5 mg/mL, no propulsion can be observed at any frequency for 100 Oe fields.

The nanoscrews, in addition to displaying a higher step-out frequency than the larger helices in the viscous medium, actually seem to experience a considerable enhancement in propulsion when moved from the viscous into the viscoelastic medium. For example, in 5 mg/mL HA, dimensionless velocities of up to 0.38 were observed at 50 Hz for individual propellers. Furthermore, the step-out frequency seems to be higher in HA solutions, because even at 80 Hz in 5 mg/mL HA, the dimensionless velocity is still significantly higher than the highest value achieved in viscous solutions. From these measurements, it appears that the nanoscrews do not experience the macroscopic viscosity of the polymer solution, as their step-out frequency does not, as would be expected in this case, decrease. At the same time the nanopropellers retain very high directionality and show high (dimensionless) velocities. The enhanced propulsion of the nanopropellers in HA solution, in comparison with the glycerol−water mixture, is likely due to (i) a higher viscosity (see the theoretical estimates below) and (ii) hindered pitching due to interaction of the nanopropeller with the entangled polymer mesh, which results in improved directionality. The latter mechanism should become operative when the length of the propeller exceeds the mesh size of an entangled polymer network.

Figure 4b shows the track of a nanopropeller in 5 mg/mL HA at 50 Hz, recorded over 70 s. Note the much higher velocity and lower noise (*i.e.*, less pitching) than the track in Figure 4a, in accord with the arguments above. A video of an ensemble of nanoscrews moving through 5 mg/mL HA can be found in the SI. We verified that quantum dot (QD) functionalization made no appreciable difference to the microscrew propulsion, indicating that the difference in dimensionless velocity

between the nano- and micropropellers is due to their size, rather than the details of their surface chemistry or morphology (see SI for details).

In the case of active propulsion of nanoparticles through a viscoelastic polymer solution, both enhanced and retarded propulsion have been predicted theoretically.[14−18] To our knowledge, however, none of these analyses were based on a model where the medium's viscoelastic properties were derived from strongly interconnected networks with the same (or slightly smaller in the case of the micropropellers) size dimensions as the propelling particles. Indeed, the reversal of relative efficiency between microhelices in the Newtonian medium and nanohelices in HA is a general consequence of the mesh network present in biological fluids. In a Newtonian fluid, the magnetic torque that can be applied to a nanopropeller and the viscous drag that opposes it both scale as L^3, where L is the characteristic particle size. Translational diffusion on the other hand scales as L^{-1}. The net result is that in a Newtonian fluid larger particles propel with improved efficiency. In the mesh network of HA, however, the resistance to motion, f, is associated with an activation barrier determined by the elastic expansion of the mesh:[24,46]

$$f \approx f_0 \exp\left(\beta\left(\frac{L}{\chi}\right)^{\delta}\right) \tag{1}$$

Here, χ is the mesh size and f_0 is the resistance in pure solvent. β approaches 1, and δ is usually assumed to be 1.[24] Since this grows much faster with size than the cubic term in the torque, it means that in biological fluids having dense networks increasing the particle size only improves efficiency for propellers up to around the critical mesh size. However, Brownian motion has the potential to render such particles uncontrollable.

A theoretical framework for the observations in viscous Newtonian liquids is provided by a simple analytical estimate of the effect of thermal noise on the propulsion of the nanoscrews. The complete analysis can be found in the SI. We consider a purely diametrically magnetized nanohelix with magnetic moment m subject to rotation by an external magnetic field of strength H and frequency ω. In the absence of Brownian diffusion and in the synchronous high-frequency regime,[47] the propeller frequency matches that of the magnetic field, $\Omega_3 = \omega$, and the helix's axis is aligned with the rotation axis of the field ($\theta \approx 0$). Rotation−translation coupling leads to translational velocity U_Z.

The addition of thermal noise may affect the motion *via* three different mechanisms: (i) hindering of the forced rotation about the axis, thus effectively reducing Ω_3 (*i.e.*, *via* rotational diffusion about the helix axis); (ii) hindering the propulsion *via* translational diffusion along the axis, which perturbs U_Z; and (iii) reduction of directionality by introducing misalignment in θ, the angle the axis of the helix makes with the rotation axis of the field (*via* rotational diffusion of the helical axis).

All of the above mechanisms are characterized by their respective Péclet numbers (Pe), which compare the relative importance of the driving force to the noise. The criterion for the minimal size of a propeller can be derived from the condition that Pe = 1, at which point diffusion becomes equal to the rate of directed motion. Note that mechanisms (i) and (ii) directly affect the propulsion speed, but not the directionality, while (iii) affects the directionality or steerability.

The Pe numbers for mechanisms (i), (ii), and (iii) are, respectively,

$$\mathrm{Pe}_{\mathrm{r}}^{\parallel} = \frac{\Omega_3}{D_{\mathrm{r}}^{\parallel}}, \quad \mathrm{Pe}_{\mathrm{t}} = \frac{U_Z L}{D_{\mathrm{t}}}, \quad \mathrm{Pe}_{\mathrm{r}}^{\perp} = \frac{1}{D_{\mathrm{r}}^{\perp}\tau_{\mathrm{rel}}} \tag{2}$$

where $D_{\mathrm{r}}^{\parallel}$, D_{t}, and $D_{\mathrm{r}}^{\perp}$ are respectively the diffusivity coefficients for rotation about, translation along, and rotation perpendicular to the helical axis. τ_{rel} is the typical relaxation time of the helix toward the magnetic field axis. Based on these, it is possible to determine the critical helix length, above which the external driving force is more important than the noise, for each of the three modes of perturbation (see SI for further information):

$$L_{\mathrm{r}*}^{\parallel} \simeq \left(\frac{k_{\mathrm{B}}T}{\tilde{\kappa}_{\parallel}\eta\omega}\right)^{1/3} \tag{3}$$

$$L_{\mathrm{t}^*} \simeq \left(\frac{k_{\mathrm{B}}T}{\tilde{B}_{\parallel}\eta\omega}\right)^{1/3} \tag{4}$$

$$L_{\mathrm{r}*}^{\perp} = \left(\frac{2k_{\mathrm{B}}T}{\tilde{\kappa}_{\parallel}\eta\sqrt{\omega_{\mathrm{s\text{-}o}}^2 - \omega^2}}\right)^{1/3} \tag{5}$$

Here η is the dynamic viscosity of the liquid, $\tilde{\kappa}_{\parallel}$ is the dimensionless rotational resistance, $\tilde{B}_{\parallel}$ is the dimensionless coupling viscous resistance coefficient, $\omega_{\mathrm{s\text{-}o}}$ is the step-out frequency, and k_{B} and T are the Boltzmann constant and temperature, respectively. The coefficients $\tilde{B}_{\parallel}$ and $\tilde{\kappa}_{\parallel}$ depend solely on the shape of the propeller and are independent of its size. Increasing the viscosity reduces the critical length and thus permits smaller helices to be actuated. However, the critical length associated with steerability $L_{\mathrm{r}*}^{\perp}$ is not affected by the fluid viscosity at frequencies significantly below the step-out frequency, where we obtain a simple condition for the steerability (see SI for details):

$$\mathrm{Pe}_{\mathrm{r}*}^{\perp} \approx \frac{mH}{2k_{\mathrm{B}}T} > 1 \tag{6}$$

Given the geometry of the nanohelices and driving frequency, one can estimate $L_{\mathrm{r}*}^{\perp}$ and $L_{\mathrm{t}*}$ in eqs 3 and 4. For a four-turn screw with a helix to filament radius ratio

of $R/r \approx 1$ (where r is the filament diameter), we find numerically that $\tilde{\kappa}_{\parallel} \simeq 0.18$ and $\tilde{B}_{\parallel} \simeq 0.011$. Thus, in water ($\eta = 1$ cP) we obtain $L^{\parallel}_{r^*} \approx 420$ nm and $L_{t^*} \approx 1060$ nm for a driving frequency of $\nu = \omega/2\pi = 50$ Hz. These estimates support the experimental observations indicating that thermal fluctuations hinder propulsion of the nanoscrews in water. Increasing the viscosity to $\eta = 25$ cP, the critical lengths are reduced to $L^{\parallel}_{r^*} \approx 140$ nm and $L_{t^*} = 360$ nm. Note that this value increases if the frequency is decreased, which is why no effective propulsion is determined at a frequency of 10 Hz (as opposed to the micropropellers, see Table 1). Turning to the steerability, using $m \approx 2 \times 10^{-14}$ emu from the SQUID measurements (estimated by dividing the magnetization by the surface density of helices) and the amplitude of the anisotropy field $H_a = 65$ Oe (see SI for details), we obtain $\mathrm{Pe}^{\perp}_{r^*} \approx 32$, consistent with the observed steerability of our nanopropellers. Based on this, eq 5 suggests that ω can approach 99% of the step-out frequency before the Péclet number drops below 1 and steerability is lost.

CONCLUSION

Artificial micropropellers that can be actuated and controlled with high precision are an active field of research, and many interesting biomedical applications have been envisioned for them. Until now, however, existing "microrobots" faced problems with actuation in biological fluids, which display complex rheological properties due to the presence of polymeric macromolecular networks. Furthermore, for applications at or in cells much smaller nanoscale hybrid propellers are needed, which could thus far not be fabricated.

In this work we present solutions to both of these issues. We report what we believe are the smallest magnetically actuated helical propellers that have been fabricated to date. The nanopropellers are small enough to be controllably navigated through the macromolecular mesh of biological fluids or gels. We analyzed their propulsion behavior and thermal noise contribution in viscous solutions both theoretically and experimentally. With a magnetic layer of thickness 40 nm and width of less than 120 nm, the nanoscrews are ferromagnetic with a higher diametrical than axial permeability, and they are able to propel in solutions with a viscosity of about 25 cP. In water, our observations and theoretical analysis confirm previous predictions[30] that propellers of this size are not able to overcome the thermal noise in order to achieve directional movement.

However, in hyaluronan solution, a polymeric viscoelastic gel that can be found in a large number of biological tissues, we show that nanoscrews can be actively propelled. As opposed to larger micropropellers with a diameter of several hundred nanometers, the nanoscrews can move through the HA solutions and even do so with significantly higher velocities than in Newtonian fluids, such as water. This demonstrates that nanopropellers smaller than a certain threshold size determined by the microscopic structure of the surrounding medium may experience significantly enhanced propulsion efficiencies, which paves the way for actively propelled "nanorobots" inside biological media and living organisms. In addition, the nanopropellers not only are promising for applications in an extracellular environment but are even small enough for potential applications inside cells.

METHODS

Solutions with a viscosity of approximately 25 cP were prepared using glycerol (99.5%, VWR) and water according to the parametrization proposed by Cheng.[48] Hyaluronic acid sodium salt from *Streptococcus equi* was purchased from Sigma-Aldrich. HA solutions were prepared by shaking a mixture of phosphate buffer (50 mM, pH 5.8), in which magnetic helices were dispersed, and the appropriate amount of HA at 4 °C for at least 12 h.

The magnetic nanoscrews were fabricated using the nanoGLAD technique described previously.[32] The Au-dot spacing on the wafers was around 135 nm, and they were enlarged in a first GLAD step using SiO_2 before depositing the Ni-layer. The deposition was carried out at room temperature. The fabrication of the micropropellers and the magnetization of the samples are described elsewhere.[38]

SQUID measurements were taken of wafer pieces in plane and out of plane at 300 K using a Quantum Design MPMS magnetometer.

For the quantum-dot functionalization, a piece of the wafer was suspended in a solution of 15 μL of (3-mercaptopropyl)-trimethoxysilane (95%, Sigma-Aldrich) in 1 mL of toluene (for analysis, Merck) for 2 h at room temperature. After washing with toluene, the wafer was then immersed in a solution of 0.25 mg/mL Lumidot CdSe 640 (Sigma-Aldrich) in toluene. The vial was purged with Ar, sealed, and left to react at room temperature overnight. The sample was then washed with toluene and dried under N_2. For fluorescence imaging, excitation was carried out at 385 nm.

For the propulsion studies, a magnetic field strength of about 100 Oe and frequencies between 10 and 80 Hz were applied using a previously described water-cooled three-axis Helmholtz coil system.[38] We used a Zeiss Observer Z1 with an AxioCam MRm camera and a minimum pixel resolution of 5 pixels/μm. All experiments were carried out at room temperature. For the velocity measurements, the particles were tracked for a minimum of 20 s (15 s if the velocity exceeded 3 μm/s). For each condition (medium, frequency) the results from at least 20 particles were averaged.

Conflict of Interest: The authors declare no competing financial interest.

Supporting Information Available: Discussion of surface chemistry effects, derivation of the critical propeller lengths, and videos of propelling nanohelices. This material is available free of charge *via* the Internet at http://pubs.acs.org.

Acknowledgment. We thank the Department Schütz, Max-Planck-Institute for Intelligent Systems, for access to the SQUID magnetometer, the Department Spatz, Max-Planck-Institute for Intelligent Systems, for SEM access and micellar nanolithography support, as well as A. Posada for help with

producing Figure 1, and the Max Planck Society for financial support. This work was in part supported by the European Research Council under the ERC Grant agreement 278213 (D.S., A.M., J.G., C.M., and P.F.), by Rubin Scientific and Medical Research Fund (A.L.), the Israel Ministry for Immigrant Absorption (K.M.), and the German Israeli Foundation (K.M., A.L., P.F.).

REFERENCES AND NOTES

1. Ghosh, A.; Fischer, P. Controlled Propulsion of Artificial Magnetic Nanostrucutred Propellers. *Nano Lett.* **2009**, *9*, 2243–2245.
2. Gao, W.; Feng, X.; Pei, A.; Kane, C. R.; Tam, R.; Hennessy, C.; Wang, J. Bioinspired Helical Microswimmers Based on Vascular Plants. *Nano Lett.* **2014**, *14*, 305–310.
3. Tottori, S.; Zhang, L.; Peyer, K. E.; Nelson, B. J. Assembly, Disassembly, and Anomalous Propulsion of Microscopic Helices. *Nano Lett.* **2013**, *13*, 4263–4268.
4. Ghosh, A.; Paria, D.; Singh, H. J.; Venugopalan, P. L.; Ghosh, A. Dynamical Configurations and Bistability of Helical Nanostructures under External Torque. *Phys. Rev. E* **2012**, *86*, 031401.
5. Keaveny, E. E.; Walker, S. W.; Shelley, M. J. Optimization of Chiral Structures for Microscale Propulsion. *Nano Lett.* **2013**, *13*, 531–537.
6. Qiu, F.; Zhang, L.; Peyer, K. E.; Casarosa, M.; Franco-Obregón, A.; Choi, H.; Nelson, B. J. Noncytotoxic Artificial Bacterial Flagella Fabricated from Biocompatible ORMOCOMP and Iron Coating. *J. Mater. Chem. B* **2014**, *2*, 357–362.
7. Ozin, G. A.; Manners, I.; Fournier-Bidoz, S.; Arsenault, A. Dream Nanomachines. *Adv. Mater.* **2005**, *17*, 3011–3018.
8. Vig, D. K.; Wolgemuth, C. W. Swimming Dynamics of the Lyme Disease Spirochete. *Phys. Rev. Lett.* **2012**, *109*, 218104.
9. Kimsey, R. B.; Spielman, A. Motility of Lyme Disease Spirochetes in Fluids as Viscous as the Extracellular Matrix. *J. Infect. Dis.* **1990**, *162*, 1205–1208.
10. Berg, H. C.; Turner, L. Movement of Microorganisms in Viscous Environment. *Nature* **1979**, *278*, 349–351.
11. Suarez, S. S.; Dai, X. Hyperactivation Enhances Mouse Sperm Capacity for Penetrating Viscoelastic Media. *Biol. Reprod.* **1992**, *46*, 686–691.
12. Shen, X. N.; Arratia, P. E. Undulatory Swimming in Viscoelastic Fluids. *Phys. Rev. Lett.* **2011**, *106*, 208101.
13. Celli, J. P.; Turner, B. S.; Afdhal, N. H.; Keates, S.; Ghiran, I.; Kelly, C. P.; Ewoldt, R. H.; McKinley, G. H.; So, P.; Erramilli, S.; *et al*. *Heliobacter Pylori* Moves through Mucus by Reducing Mucin Viscoelasticity. *Proc. Natl. Acad. Sci. U.S.A.* **2009**, *106*, 14321.
14. Liu, B.; Powers, T. R.; Breuer, K. S. Force-Free Swimming of a Model Helical Flagellum in Viscoelastic Fluids. *Proc. Natl. Acad. Sci. U.S.A.* **2011**, *108*, 19516–19520.
15. Spagnolie, S. E.; Liu, B.; Powers, T. R. Locomotion of Helical Bodies in Viscoelastic Fluids: Enhanced Swimming at Large Helical Amplitudes. *Phys. Rev. Lett.* **2013**, *111*, 068101.
16. Leshansky, A. M. Enhanced Low-Reynolds-Number Propulsion in Heterogeneous Viscous Environments. *Phys. Rev. E* **2009**, *80*, 051911.
17. Fu, H. C.; Wolgemuth, C. W.; Powers, T. R. Swimming Speeds of Filaments in Nonlinearly Viscoelastic Fluids. *Phys. Fluids* **2009**, *21*, 033102.
18. Fu, H. C.; Shenoy, V. B.; Powers, T. R. Low-Reynolds-Number Swimming in Gels. *EPL* **2010**, *91*, 24002.
19. Venugopalan, P. L.; Sai, R.; Chandorkar, Y.; Basu, B.; Shivashankar, S.; Ghosh, A. Conformal Cytocompatible Ferrite Coatings Facilitate the Realization of a Nanovoyager in Human Blood. *Nano Lett.* **2014**, *14*, 1968–1975.
20. Strous, G. J.; Dekker, J. Mucin-Type Glycoproteins. *Crit. Rev. Biochem. Mol. Biol.* **1992**, *27*, 57–92.
21. Sharif-Kashani, P.; Hubschman, J.-P.; Sassoon, D.; Kavehpour, H. P. Rheology of the Vitreous Gel: Effects of Macromolecule Organization on the Viscoelastic Properties. *J. Biomech.* **2011**, *44*, 419.
22. Kogan, G.; Soltés, L.; Stern, R.; Gemeiner, P. Hyaluronic Acid: A Natural Biopolymer with a Broad Range of Biomedical and Industrial Applications. *Biotechnol. Lett.* **2007**, *29*, 17–25.
23. Masuda, A.; Ushida, K.; Koshino, H.; Yamashita, K.; Kluge, T. Novel Distance Dependence of Diffusion Constants in Hyaluronan Aqueous Solution Resulting from its Characteristic Nano-Microstructure. *J. Am. Chem. Soc.* **2001**, *123*, 11468–11471.
24. De Smedt, S. C.; Lauwers, A.; Demeester, J.; Engelborghs, Y.; De Mey, G.; Du, M. Structural Information on Hyaluronic Acid Solutions As Studied by Probe Diffusion Experiments. *Macromolecules* **1994**, *27*, 141–146.
25. Xu, Q.; Boylan, N. J.; Suk, J. S.; Wang, Y.-Y.; Nance, E. A.; Yang, J.-C.; McDonnell, P. J.; Cone, R. A.; Duh, E. J.; Hanes, J. Nanoparticle Diffusion in, and Microrheology of, the Bovine Vitreous ex Vivo. *J. Controlled Release* **2013**, *167*, 76–84.
26. Kirch, J.; Schneider, A.; Abou, B.; Hopf, A.; Schaefer, U. F.; Schneider, M.; Schall, C.; Wagner, C.; Lehr, C.-M. Optical Tweezers Reveal Relationship between Microstructure and Nanoparticle Penetration of Pulmonary Mucus. *Proc. Natl. Acad. Sci. U.S.A.* **2012**, *109*, 18355–18360.
27. Tammi, M. I.; Day, A. J.; Turley, E. A. Hyaluronan and Homeostasis: A Balancing Act. *J. Biol. Chem.* **2002**, *277*, 4581–4584.
28. Day, A. J.; Prestwich, G. D. Hyaluronan-Binding Proteins: Tying Up the Giant. *J. Biol. Chem.* **2002**, *277*, 4585–4588.
29. Cowman, M. K.; Matsuoka, S. Experimental Approaches to Hyaluronan Structure. *Carbohydr. Res.* **2005**, *340*, 791–809.
30. Ghosh, A.; Paria, D.; Rangarajan, G.; Ghosh, A. Velocity Fluctuations in Helical Propulsion: How Small Can a Propeller Be. *J. Phys. Chem. Lett.* **2014**, *5*, 62–68.
31. Nance, E. A.; Woodworth, G. F.; Sailor, K. A.; Shih, T.-Y.; Xu, Q.; Swaminathan, G.; Xiang, D.; Eberhart, C.; Hanes, J. A Dense Poly(ethylene glycol) Coating Improves Penetration of Large Polymeric Nanoparticles within Brain Tissue. *Sci. Trans. Med.* **2012**, *4*, 149ra119.
32. Mark, A. G.; Gibbs, J. G.; Lee, T.-C.; Fischer, P. Hybrid Nanocolloids with Programmed Three-Dimensional Shape and Material Composition. *Nat. Mater.* **2013**, *12*, 802–807.
33. Zhao, Y. P.; Ye, D. X.; Wang, G. C.; Lu, T. M. Novel Nano-Column and Nano-Flower Arrays by Glancing Angle Deposition. *Nano Lett.* **2002**, *2*, 351–354.
34. Hawkeye, M.; Brett, M. J. Glancing Angle Deposition: Fabrication, Properties, and Applications of Micro- and Nanostructured Thin Films. *J. Vac. Sci. Technol. A* **2007**, *25*, 1317–1335.
35. Robbie, K.; Brett, M. J.; Lakhtakia, A. Chiral Sculptured Thin Films. *Nature* **1996**, *384*, 616.
36. Gibbs, J.; Mark, A. G.; Lee, T.-C.; Eslami, S.; Schamel, D.; Fischer, P. Nanohelices by Shadow Growth. *Nanoscale* **2014**, 10.1039/C4NR00403E.
37. Glass, R.; Möller, M.; Spatz, J. P. Block Copolymer Micelle Nanolithography. *Nanotechnology* **2003**, *14*, 1153–1160.
38. Schamel, D.; Pfeifer, M.; Gibbs, J. G.; Miksch, B.; Mark, A. G.; Fischer, P. Chiral Colloidal Molecules and Observation of the Propeller Effect. *J. Am. Chem. Soc.* **2013**, *135*, 12353–12359.
39. Janssen, X. J. A.; Schellekens, A. J.; van Ommering, K.; van Ijzendoorn, L. J.; Prins, M. W. J. Controlled Torque on Superparamagnetic Beads for Functional Biosensors. *Biosens. Bioelectron.* **2009**, *24*, 1937–1941.
40. De Smedt, S. C.; Dekeyser, P.; Ribitsch, V.; Lauwers, A.; Demeester, J. Viscoelastic and Transient Network Properties of Hyaluronic Acid as a Function of the Concentration. *Biorheology* **1993**, *30*, 31–41.
41. Kobayashi, Y.; Okamoto, A.; Nishinari, K. Viscoelasticity of Hyaluronic Acid with Different Molecular Weights. *Biorheology* **1994**, *31*, 235–244.
42. Nijenhuis, N.; Mizuno, D.; Schmidt, C. F.; Vink, H.; Spaan, J. A. E. Microrheology of Hyaluronan Solutions: Implications for the Endothelial Glycocalyx. *Biomacromolecules* **2008**, *9*, 2390–2398.

43. Scott, J. E.; Cummings, C.; Brass, A.; Chen, Y. Secondary and Tertiary Structures of Hyaluronan in Aqueous Solution, Investigated by Rotary Shadowing-Electron Microscopy and Computer Simulation. *Biochem. J.* **1991**, *274*, 699–705.
44. Fouissac, E.; Milas, M.; Rinaudo, M.; Borsali, R. Influence of the Ionic Strength on the Dimensions of Sodium Hyaluronate. *Macromolecules* **1992**, *25*, 5613–5617.
45. Krause, W. E.; Bellomo, E. G.; Colby, R. H. Rheology of Sodium Hyaluronate under Physiological Conditions. *Biomacromolecules* **2001**, *2*, 65–69.
46. de Gennes, P.-G. *Scaling Concepts in Polymer Physics*; Cornell University Press: Ithaca, NY, 1979.
47. Morozov, K. I.; Leshansky, A. M. The Chiral Magnetic Nanomotors. *Nanoscale* **2014**, *6*, 1580–1588.
48. Cheng, N.-S. Formula for the Viscosity of a Glycerol-Water Mixture. *Ind. Eng. Chem. Res.* **2008**, *47*, 3285–3288.